AD-A241 551

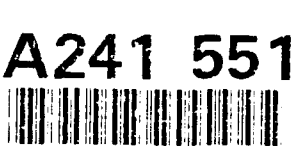

TECHNICAL REPORT BRL-TR-3269

BRL

PREDICTING DYNAMIC STRAIN AMPLIFICATION BY COUPLING A FINITE ELEMENT STRUCTURAL ANALYSIS CODE WITH A GUN INTERIOR BALLISTIC CODE

DTIC
ELECTE
OCT 15 1991
S B D

DAVID A. HOPKINS

SEPTEMBER 1991

APPROVED FOR PUBLIC RELEASE; DISTRIBUTION IS UNLIMITED.

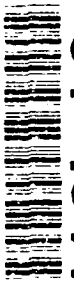

91-13149

U.S. ARMY LABORATORY COMMAND

BALLISTIC RESEARCH LABORATORY
ABERDEEN PROVING GROUND, MARYLAND

NOTICES

Destroy this report when it is no longer needed. DO NOT return it to the originator.

Additional copies of this report may be obtained from the National Technical Information Service, U.S. Department of Commerce, 5285 Port Royal Road, Springfield, VA 22161.

The findings of this report are not to be construed as an official Department of the Army position, unless so designated by other authorized documents.

The use of trade names or manufacturers' names in this report does not constitute indorsement of any commercial product.

UNCLASSIFIED

REPORT DOCUMENTATION PAGE

Form Approved
OMB No. 0704-0188

Public reporting burden for this collection of information is estimated to average 1 hour per response, including the time for reviewing instructions, searching existing data sources, gathering and maintaining the data needed, and completing and reviewing the collection of information. Send comments regarding this burden estimate or any other aspect of this collection of information, including suggestions for reducing this burden, to Washington Headquarters Services, Directorate for information Operations and Reports, 1215 Jefferson Davis Highway, Suite 1204, Arlington, VA 22202-4302, and to the Office of Management and Budget, Paperwork Reduction Project (0704-0188), Washington, DC 20503

1. AGENCY USE ONLY (Leave blank)	2. REPORT DATE	3. REPORT TYPE AND DATES COVERED
	September 1991	Final, Aug 90 - Dec 90

4. TITLE AND SUBTITLE

Predicting Dynamic Strain Amplification by Coupling a Finite Element Structural Analysis Code With a Gun Interior Ballistic Code

5. FUNDING NUMBERS

PR: 1L162618AH80

6. AUTHOR(S)

David A. Hopkins

7. PERFORMING ORGANIZATION NAME(S) AND ADDRESS(ES)

8. PERFORMING ORGANIZATION REPORT NUMBER

9. SPONSORING / MONITORING AGENCY NAME(S) AND ADDRESS(ES)

U.S. Army Ballistic Research Laboratory
ATTN: SLCBR-DD-T
Aberdeen Proving Ground, MD 21005-5066

10. SPONSORING / MONITORING AGENCY REPORT NUMBER

BRL-TR-3269

11. SUPPLEMENTARY NOTES

12a. DISTRIBUTION / AVAILABILITY STATEMENT

Approved for public release; distribution is unlimited.

12b. DISTRIBUTION CODE

13. ABSTRACT *(Maximum 200 words)*

The dynamic strain amplification effect caused by a traveling pressure front in a gun tube is examined by coupling a hydrodynamic finite element code, DYNA2D, with an interior ballistic code, IBRGAC. Results are presented comparing the circumferential stress response predictions for a pressure front traveling at constant velocity in a constant cross-section tube with theoretical results. Next, the response due to an accelerating pressure front is examined. Finally, the circumferential stress response due to an M829 projectile fired from an M256 tank cannon is determined using the coupled code.

14. SUBJECT TERMS

interior ballistics; stress analysis; finite element analysis; traveling load

15. NUMBER OF PAGES

21

16. PRICE CODE

17. SECURITY CLASSIFICATION OF REPORT	18. SECURITY CLASSIFICATION OF THIS PAGE	19. SECURITY CLASSIFICATION OF ABSTRACT	20. LIMITATION OF ABSTRACT
UNCLASSIFIED	UNCLASSIFIED	UNCLASSIFIED	UL

INTENTIONALLY LEFT BLANK.

TABLE OF CONTENTS

DTIC COPY INSPECTED

Accession For
NTIS GRA&I
DTIC TAB
Unannounced
Justification
By
Distribution/
Availability Codes
Dist Special
A-1

INTENTIONALLY LEFT BLANK.

LIST OF FIGURES

LIST OF TABLES

INTENTIONALLY LEFT BLANK.

1. INTRODUCTION

The successful design of gun tubes and projectiles relies upon the ability to accurately predict the stresses and strains induced in these structures by the applied loads. These applied loads include the internal pressurization of the tube, the body force loads in the projectile due to its acceleration by the base pressure, and loads caused by interaction between the projectile and the gun tube during shot travel. The calculation of the stresses induced in the projectile by the base pressure is straightforward using existing finite element (FE) codes (Bannister 1989; Kaste and Wilkerson, to be published). Similarly, Lamé's equations for the stresses induced in a tube due to internal pressurization (Timoshenko and Goodier 1951) are routinely employed in the design of gun tubes based on the maximum pressure profile. However, loads induced by interaction between the gun tube and the projectile are still not fully accounted for in design practice. In particular, the effect of a traveling pressure front on the stresses induced in a gun tube have only recently regained attention as an important aspect of the design problem.

The effect of a traveling pressure front on the stresses and strains in a constant cross section, infinite length tube was initially investigated by Taylor (1942). More recently, Simkins (1987, 1989) has completed a more detailed and accurate analytic analysis of this problem using the theory of elasticity. These analyses indicate that as the velocity of the pressure front increases, the strains, and consequently the stresses, induced in the tube can be amplified substantially above the strains determined by a simple static analysis based on Lamé's equations. This amplification is caused by the velocity of the pressure front approaching a resonance velocity in the tube. This effect is referred to as dynamic strain amplification in this report. This effect has significant influence upon the design of gun tubes since designs based on the maximum pressure profile may be inadequate for cases where the projectile approaches this resonance velocity.

For complicated structures, modern structural analysis methods use FE techniques. Prediction of the effects of a moving pressure front on the strains in a tube using FE models have been successful but only after considerable effort in determining how the loads due to the pressure front are applied to the model. The current state of the methods used is such that the inclusion of a traveling pressure front in a realistic model of a gun tube firing a

projectile is still a formidable task. Also, the simple application of a pressure to the tube as the projectile travels down-bore overlooks the tube/projectile interaction problem and how this interaction may affect the pressure front. To see this more clearly, it is worth reexamining current practice.

The pressure acting on the base of a projectile is obtained either from experimental data or, as is more common, by using a gun interior ballistics computer code (Robbins and Raab 1988; Gough, to be published) to compute the expected pressure loads. This pressure-time history is then used to define the loads acting on the base of the projectile in the FE model of the gun tube and projectile. However, because the pressure load curve already includes some effects caused by projectile/tube interaction such as friction, these effects should not be included in the FE model. Consequently, the FE model normally assumes a frictionless interface between the projectile and gun tube. For most analyses, this approach is entirely adequate in determining the dominant loads acting on the projectile.

Such is not the situation for dynamic simulations of gun tubes using finite element models. The gun tube is normally not subjected to internal pressurization in these structural analyses. This pressurization can be included in current FE models by specifying a pressure-time history for every element on the interior face of the gun tube. For detailed models, this potentially requires specifying hundreds of load curves, one for each pressure loaded element. This can be an overly burdensome task. Recent work by Rabern and Lewis (1990) circumvents this problem by using the capabilities of the structural dynamics codes PRONTO2D and PRONTO3D to track the location of the wetted surface of the gun tube and, consequently, elements to which pressure should be applied. The wetted surface is the portion of the gun tube behind the projectile which is subjected to pressurization due to the burning propellant. This region changes as the projectile moves. However, any tube/projectile interaction effects as computed by these FE codes cannot modify the pressure time history which still serves as input to their procedure.

To address the problem of projectile/tube interaction and its effect upon the developing pressure profile, another approach has been undertaken in which a gun interior ballistics computer code, IBRGAC, and a structural dynamics FE analysis code, DYNA2D (Hallquist 1987), have been modified such that the pressure profile and the structural dynamic

response develop simultaneously, and thus are able to influence each other. Furthermore, the tube pressurization effects are included in the analysis using the capabilities of DYNA2D to track the wetted surface. In this report, a general description of the implementation of this method is discussed in the next section. Following this discussion, the capabilities of the implementation are examined using three example problems. In the first, the numerical predictions of the coupled code for the constant velocity, constant pressure traveling load problem is examined. This simple problem allows the implementation of the slide line loading algorithm to be checked and also tests the ability of the FE model to capture the dynamic strain amplification effect. In the second example, the effect of an accelerating pressure load is examined. The coupling of the FE analysis software and the interior ballistics code are checked by this example. Finally, the response of the M256 tank cannon firing an M829 kinetic energy projectile is examined. This example demonstrates that dynamic strain amplification effects are present in currently fielded weapon systems.

2. IMPLEMENTATION

Details of the coupling of the interior ballistics code IBRGAC and the structural dynamics finite element code DYNA2D will be presented in a future report. However, a brief outline of the method employed is presented in this section. The basic problem in coupling DYNA2D and IBRGAC involves the sharing of parameters such as projectile mass and rigid body displacement and velocity from the former and the base and breech pressures from the latter. These quantities must be shared by the codes in order to continue the computation at each time step. DYNA2D uses the base and breech pressures to compute the pressure loads on the projectile base and the wetted surface of the tube while IBRGAC uses the projectile mass, rigid body displacement, and rigid body velocity to update the interior pressure profile. An outline of the process is shown in Figure 1. At each time step, the DYNA2D time step algorithm calls the IBRGAC code. IBRGAC is supplied with the current estimates of the projectile's displacement, velocity, and mass, along with the desired time step size. IBRGAC uses this information together with other parameters relevant only to the interior ballistics model to compute the projectile base pressure and the tube breech pressure at the end of the time step. These values are then returned to DYNA2D. A special slide line algorithm is subsequently used by DYNA2D to compute the actual pressure loads acting on the base of the projectile and on the wetted surface of the gun tube. Given this information, the

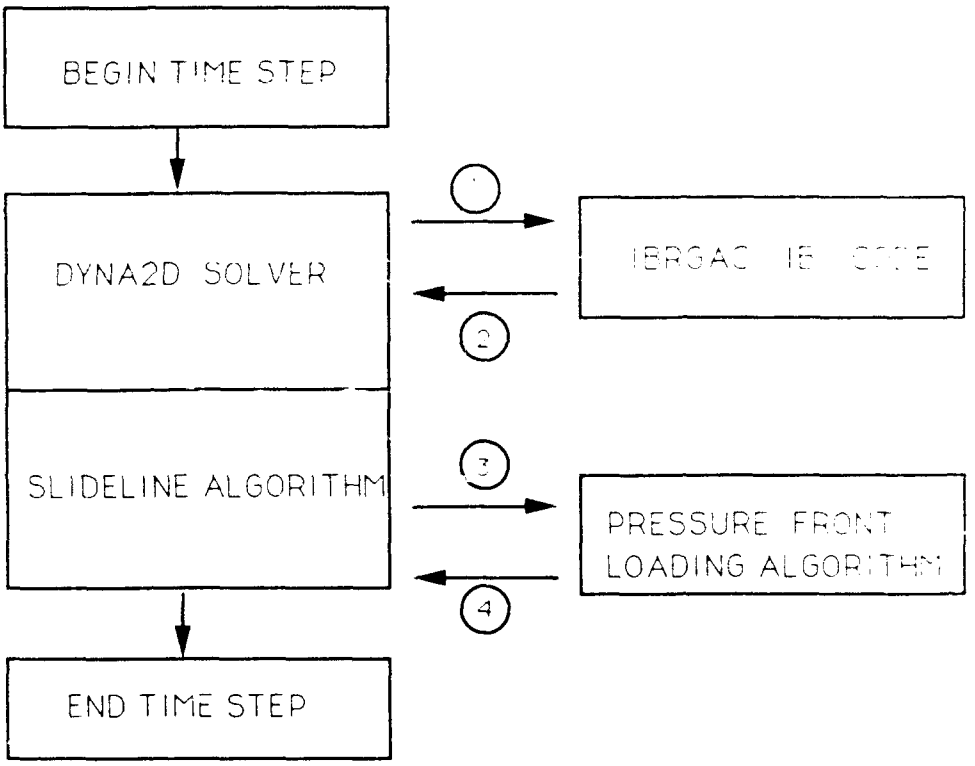

Figure 1. Flow Chart for Coupling of DYNA2D and IBRGAC.

time-stepping algorithm proceeds to the next time step. Thus, IBRGAC is basically treated as a load generation subroutine which is called by DYNA2D.

At present, this implementation cannot handle frictional sliding between the projectile and tube and thus has the same limitations as the implementations referenced earlier. However, the capability of running the interior ballistics model and the structural analysis model in tandem has been demonstrated, and work is continuing to remove the frictionless interface limitation. Removal of this restriction will allow realistic modeling of the traveling pressure front problem.

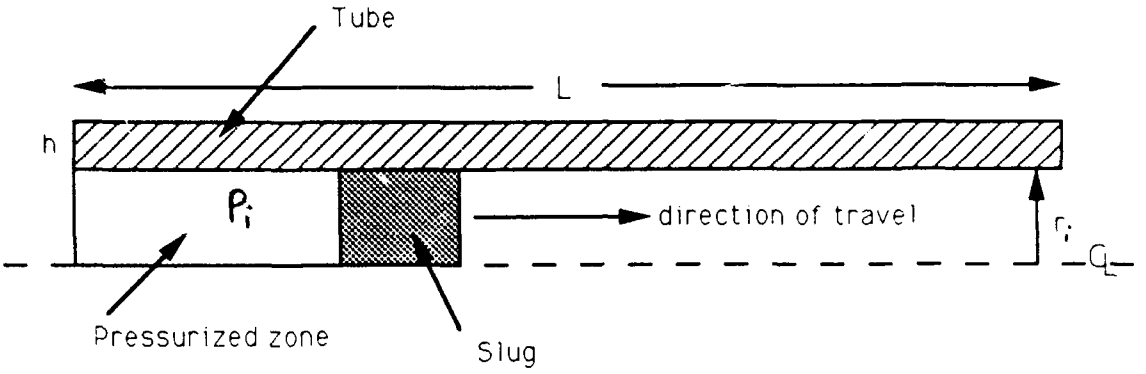

Figure 2. Simple Tube/Projectile Model Geometry.

3 RESULTS

The ability of DYNA2D to capture the dynamic strain response was verified by the use of a simple model consisting of a constant diameter tube through which a slug traveled at constant velocity (Figure 2). The wetted region of the tube was defined using the slide line capabilities of DYNA2D to track the location of the base of the slug. The diameter and thickness of the tube were selected such that the results of this test case can be compared with the results obtained by Simkins (1987, 1989). The parameters for this example are the following:

r_i = 2.36 in

h = 0.5 in

L = 200.0 in

E = 30.3 x 10^6 psi

ρ = 0.28 lb/in^3

ν = 0.3,

where r_i is the internal radius of the tube, h is the tube wall thickness, L is the tube length, E is Young's modulus, ρ is the density, and ν is Poisson's ratio.

The critical velocity, V_{cr}, at which resonance occurs, using shell theory, is given by the following:

$$V_{cr}^2 = \frac{2\left(\frac{E}{\rho}\right) h}{(2r_i + h)\sqrt{(3[1-\nu^2])}} \quad . \tag{1}$$

For the geometry of the sample problem, a critical velocity of 5,795 ft/s is obtained from Equation 1. Four constant velocity scenarios are considered. These are summarized in Table 1. The Lamé stress in the circumferential direction is calculated using Lamé's formula:

$$\sigma_\theta = \frac{P_i\, a^2}{(b^2 - a^2)}\left(1 - \frac{b^2}{r^2}\right) , \tag{2}$$

where a and b are the inner and outer radii of the tube, P_i is the internal pressure, and r is the radial location at which the circumferential stress, σ_θ, is calculated.

In Figure 3a, the circumferential stress is normalized with respect to the circumferential Lamé stress calculated at the location r = 2.4255 in. This radial location is the same location at which DYNA2D calculates the circumferential stress in an element on the inside surface of the tube, which is used for comparison in the present results. With an internal pressure of 5,870 psi, σ_θ = 29,573 psi. These stress-time curves are zeroed with respect to the time of the arrival of the pressure front. This front arrival time is given in Table 1. Examining Figure 3a, it is seen that for the low velocity case, the effect of the traveling pressure front is a slight undershoot in the hoop stress just prior to the arrival of the front, followed by a slight overshoot. The maximum hoop stress rapidly and monotonically approaches the Lamé hoop stress. In the supercritical case, V = 1.2V_{cr}, the hoop stress exhibits small oscillations prior to the arrival of the front, followed by a sustained large amplitude oscillation with a peak amplitude of approximately 2 $\sigma_{Lamé}$ after arrival of the pressure front. Both of these results are in accord with theory (Simkins 1987, 1989). However, the results near the critical velocity differ slightly from theory.

For clarity, these curves have been reproduced in Figure 3b. For V = 0.9V_{cr}, the curve resembles the predictions based on theory. However, unlike the theory, for a pressure front velocity slightly above V_{cr}, the stress response deviates from the theoretical prediction. This is

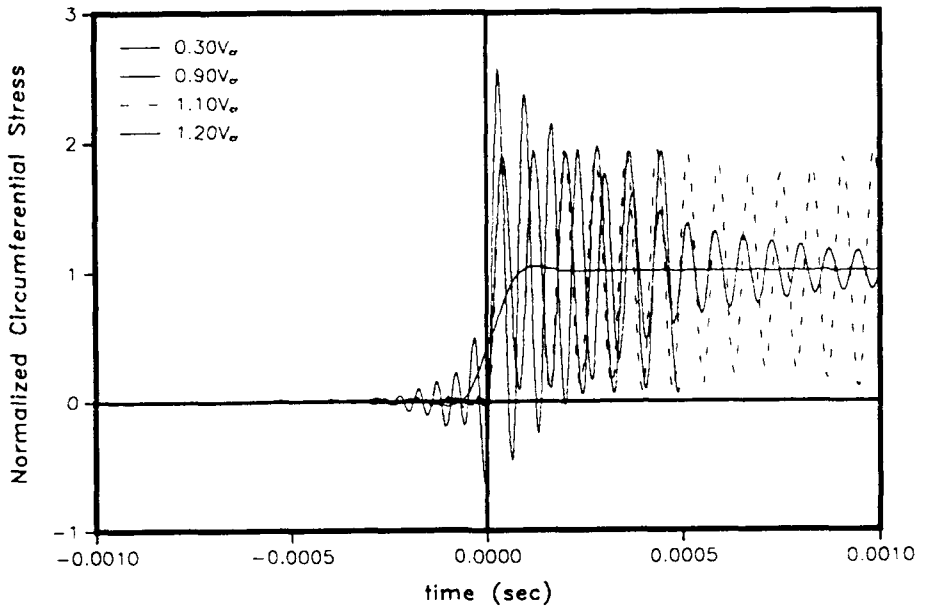

(a)

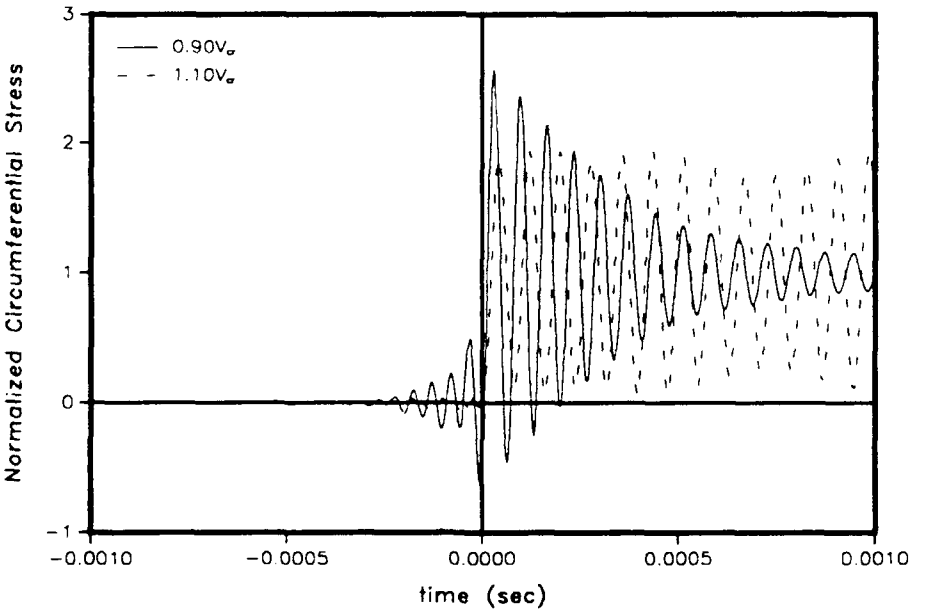

(b)

Figure 3. Normalized Circumferential Stress Response to a Constant Pressure Loading Traveling at Constant Velocity.

Table 1. Constant Pressure Front Velocity Effect on Peak Normalized Circumferential Stress

Case	V/V_{cr}	Front Velocity (in/s)[a]	Time (ms)	$\sigma_{Peak}/\sigma_{Lamé}$ [b]
1	.3	20,860	2.880	1.08
2	.9	62,590	0.962	2.75
3	1.1	76,500	0.784	2.0
4	1.2	84,840	0.710	2.0

[a] Critical velocity is 69,540 in/s (using Equation 1).
[b] Lamé stress based on pressure of 5,870 psi acting on wetted area (using Equation 2).

seen by examining the curve for $V = 1.1V_{cr}$. The response prior to front arrival appears to resemble that of the supercritical velocity case. However, after front passage, the response, while similar to the supercritical response, also exhibits a slight beating or ringing behavior. This behavior indicates that the establishment of the steady state oscillations for $V = 1.2V_{cr}$ may not be instantaneous as predicted by theory. The possibility that the response observed is due to reflection of the stress wave from the tube ends is discounted since if end reflections effects were dominant, then they should also appear in the supercritical case.

In the second problem, the effect of an accelerating projectile in a constant diameter tube upon the induced stress in the tube is examined. The purpose of this example is twofold. First, this example allows direct comparison with the results of the previous problem. Second, this example allows the effects of coupling the interior ballistic model with DYNA2D to be explored. Again, the response was examined at four locations on the tube whose velocities correspond with the velocities examined in example 1. The results are summarized in Table 2. This table lists the time of pressure front passage, pressure front velocity, axial location of the pressure front at time of interest, peak pressure at inside surface of the tube at this location, and the peak normalized circumferential stress. The stress-time histories are shown in Figure 4 in which all curves have again been zeroed with respect to passage of the pressure front. The overall shapes of the resultant stress-time histories are similar to those obtained in the constant velocity cases. However, there are some notable differences. For the low velocity curve, $V = 0.30V_{cr}$, it is seen that the stress ratio begins to rise after pressure

Table 2. Variable Pressure/Accelerating Pressure Front Effect on Peak Normalized Circumferential Stress

Case	Front Velocity (in/s)[a]	Time (ms)	Displacement (in)	Peak Pressure (psi)	$\sigma_{Peak}/\sigma_{Lamé}$ [b]
1	20,860	3.29	11.1	72,637	1.02
2	62,590	4.56	65.1	28,387	1.5
3	76,500	5.27	115.0	16,090	2.80
4	84,840	5.97	171.5	10,056	2.0

[a] Critical velocity is 69,540 in/s (using Equation 1).
[b] Lamé stress based on peak pressure acting at given location (using Equation 2).

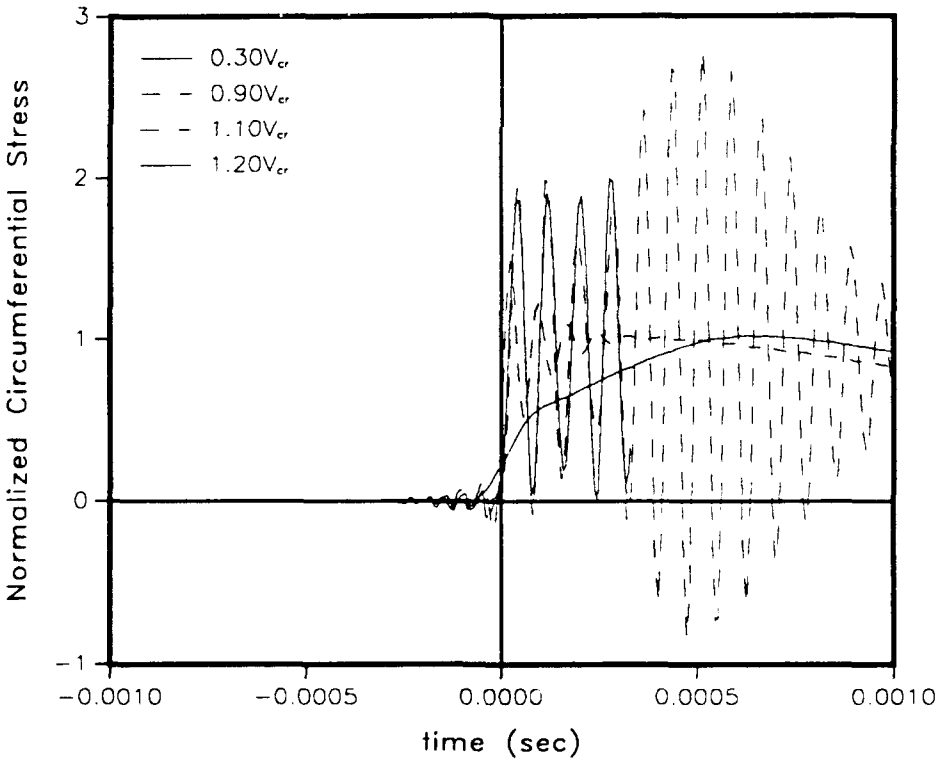

Figure 4. Normalized Circumferential Stress Response for an Accelerating, Variable Pressure Front in a Constant Cross-Section Tube.

front passage as before. However, this rise is relatively slow compared to the prior example. This difference is because peak pressure at this axial location in the tube does not occur at the time of passage of the pressure front. Consequently, it is seen that the stress increases to the value given by Lamé's formula as the pressure at this location increases then decreases as the pressure drops. Another notable difference between the constant velocity example and this one is that the maximum stress induced is due to the slightly supercritical velocity, $V = 1.1V_{cr}$; whereas, it was previously due to the slightly subcritical velocity, $V = 0.9V_{cr}$. These two curves, however, are inadequate in determining the velocity at which maximum dynamic amplification occurs. To determine this velocity, it is necessary to plot the maximum stress at all locations along the tube normalized by the maximum Lamé stress at that location. Figure 5 illustrates this effect of velocity upon the peak normalized stress. The peak normalized hoop stress is seen to initially correspond to the value given by Lamé's equation. As the projectile velocity approaches 60,000 in/s, dynamic strain amplification effects begin to influence the response. As the pressure front velocity reaches approximately 75,000 in/s, the peak normalized hoop stress reaches a maximum magnitude of approximately 2.8. After this point, as the velocity continues to increase, the steady state response with a peak magnitude of 2.0 is approached. The effect of using a finite length tube is also apparent in Figure 5. First, there is a rapid stress rise and dropoff at the ends of the tube. Second, the oscillations in the stress values may be the result of axial stress wave reflections.

The effect of the coupling of IBRGAC and DYNA2D is examined by comparing the predictions of the projectile's velocity by IBRGAC and by the coupled code. This comparison is presented in Figure 6. It is seen that while the two curves are similar, they are not identical, with the coupled code predicting a higher projectile exit velocity. Because of the formulation of the problem, it was expected that there would not be any discrepancies in the velocity predictions of the two codes. The reasons for this difference are currently under investigation. However, the maximum difference is only approximately 3% for the case considered, while the exit velocity only differs by 0.5%. Consequently, the agreement is considered excellent.

In the final example, the coupled code is used to examine the response of the M256 tank cannon firing a M829 kinetic energy round. The system geometry and finite element mesh

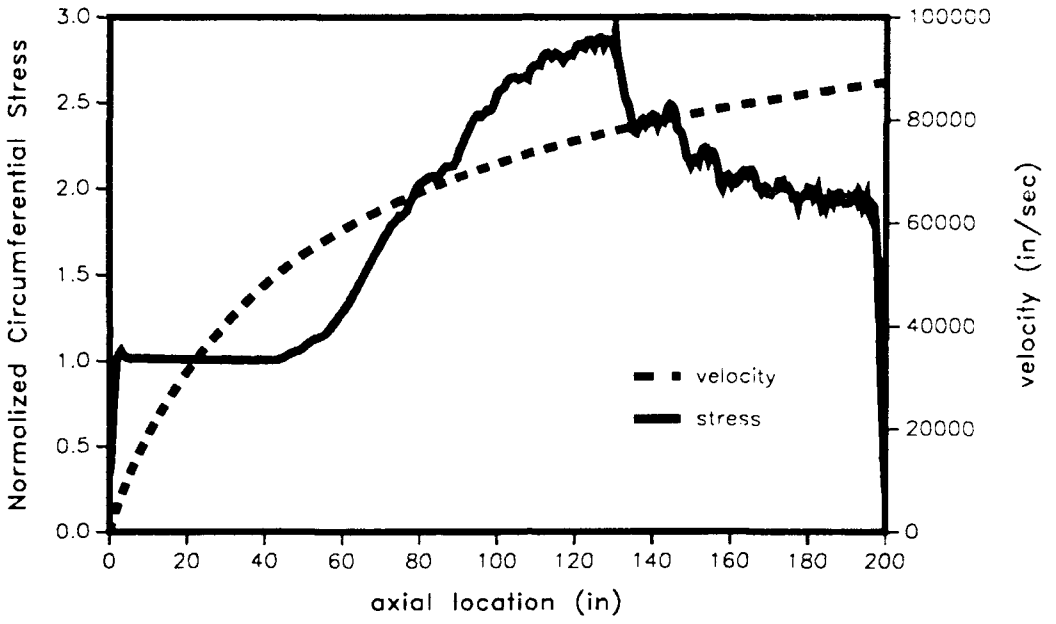

Figure 5. Peak Normalized Circumferential Stress Due to Accelerating, Variable Pressure Front and Axial Velocity vs. Axial Location.

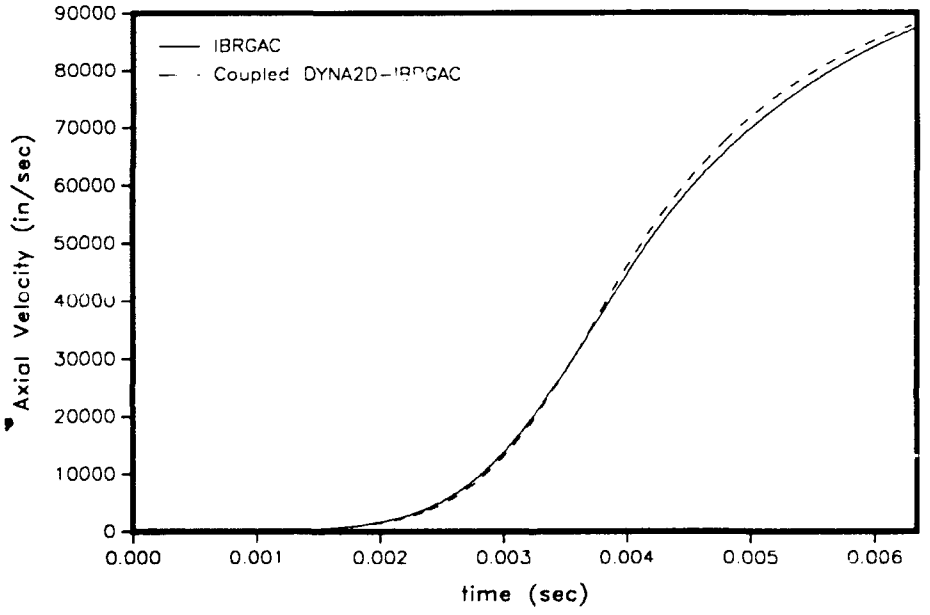

Figure 6. Comparison of Axial Velocity for the Coupled and Uncoupled Models.

are shown in Figure 7a. A close-up view of the projectile, as initially located in the tube, is shown in Figure 7b. For this example, the projectile velocity never exceeds the critical velocity for the tube. For comparison with the prior examples, two stress-time histories are shown in Figure 8 ($V = 0.66V_{cr}$, and $V = 0.73V_{cr}$). These velocities have been selected because they are representative of velocities actually achieved. These time histories clearly illustrate that dynamic strain effects are present for this system. The peak normalized hoop stress value is approximately 1.2 in Figure 8. However, as mentioned, the actual projectile velocity in this problem does not exceed the critical velocity. For this problem, the peak hoop stress will therefore occur at the thinnest tube section near the muzzle where the projectile velocity is greatest. The amplitude of this peak stress will be at least 1.2 times the value given by Equation 2. Consequently, it is possible the tube material near the muzzle may see strains and stresses above the design values, depending upon the factor of safety employed during the tube design.

4. CONCLUSIONS

The ability to model the dynamic strain amplification phenomena has been demonstrated by coupling a gun interior ballistic model with an advanced FE structural analysis model. Stress amplification predictions based on this coupled code are in agreement with theoretical results. The coupled model has been used to examine a standard gun tube, the M256, firing a standard M829 cartridge. The results indicate that for this system, the dynamic strain amplification phenomena lead to a peak stress in the tube in excess of 1.2 times the stress level determined from static calculations.

5. FUTURE WORK

Discrepancies in the predicted exit velocities of the coupled and uncoupled codes must still be resolved. Additionally, the ability to accomodate frictional sliding interfaces must be incorporated into the modeling capabilities. Finally, a more accurate representation of the pressure gradient profile acting on the wetted region behind the projectile needs to be incorporated into the model. These issues are currently under investigation.

(a)

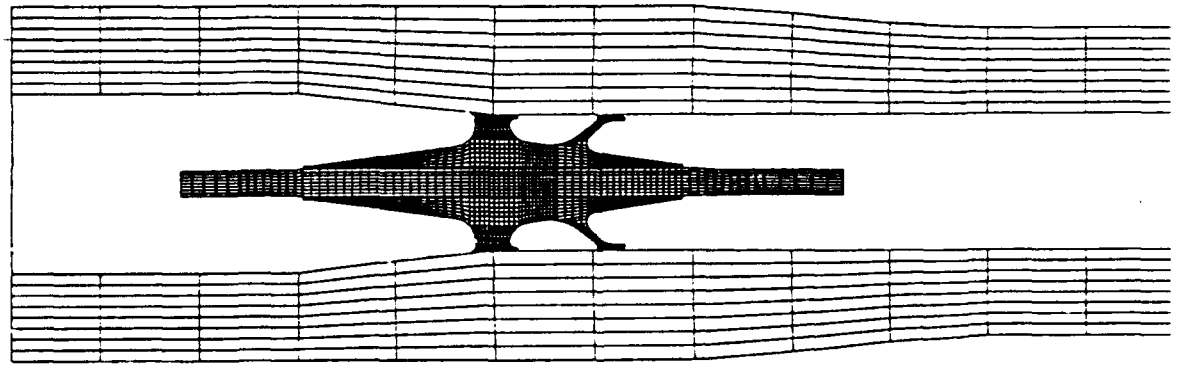

(b)

Figure 7. M256 (a) and M829 (b) System Geometry and FE Mesh.

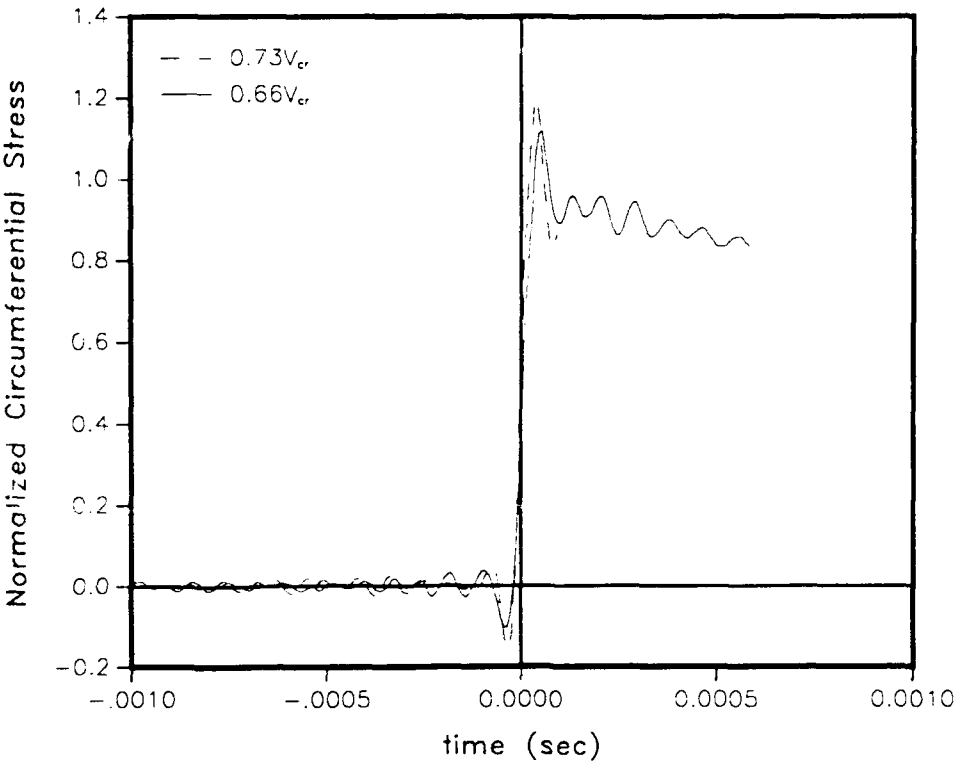

Figure 8. Effect of Projectile Velocity Upon Circumferential Stress in the M256 Gun Tube.

6. REFERENCES

Bannister, Kenneth A. "Structural Sensitivity of Saboted-Rod Projectiles to Transient In-bore Loads." Proceedings of the 11th International Symposium on Ballistics, Brussels Congress Centre, Brussels, Belgium, May 1989.

Gough, P. S. "The XNOVAKTC Code." Contract DAAK11-85-0002, to be published.

Hallquist, John O. "User's Manual for DYNA2D." Methods Development Group, Lawrence Livermore National Laboratory, Livermore, CA, February 1987.

Kaste, R. P., and S. A. Wilkerson. "An Improved Sabot Design and DYNA3D Analysis for the XM900E1 Kinetic Energy Projectile." U.S. Army Ballistic Research Laboratory, Aberdeen Proving Ground, MD, to be published.

Rabern, Donald A., and Matthew W. Lewis. "Projectile and Gun Tube Simulation With a Moving Pressure Front in Two and Three Dimensions." MEE4-90-451, Los Alamos National Laboratory, Los Alamos, NM, October 1990.

Robbins, Frederick W., and Timothy S. Raab. "A Lumped-Parameter Interior Ballistic Computer Code Using the TTCP Model." BRL-MR-3710, U.S. Army Ballistic Research Laboratory, Aberdeen Proving Ground, MD, November 1988.

Simkins, Thomas E. "Resonance of Flexural Waves in Gun Tubes." ARCCB-TR-87008, Benet Weapons Laboratory, Watervliet, NY, July 1987.

Simkins, Thomas E. "Influence of Transient Flexural Waves on Dynamic Strains in Gun Tubes." ARCCB-TR-89020, Benet Weapons Laboratory, Watervliet, NY, August 1989.

Taylor, G. I. "Strains in a Gun Barrel Near the Driving Barrel of a Moving Projectile." A.C. 1851/Gn. 104, U.K. Ministry of Supply, London, England, March 1942.

Timoshenko, S., and J. N. Goodier. Theory of Elasticity. 2d ed., New York: McGraw-Hill Book Company, Inc., 1951.

INTENTIONALLY LEFT BLANK.

USER EVALUATION SHEET/CHANGE OF ADDRESS

This laboratory undertakes a continuing effort to improve the quality of the reports it publishes. Your comments/answers below will aid us in our efforts.

1. Does this report satisfy a need? (Comment on purpose, related project, or other area of interest for which the report will be used.) _____

2. How, specifically, is the report being used? (Information source, design data, procedure, source of ideas, etc.) _____

3. Has the information in this report led to any quantitative savings as far as man-hours or dollars saved, operating costs avoided, or efficiencies achieved, etc? If so, please elaborate. _____

4. General Comments. What do you think should be changed to improve future reports? (Indicate changes to organization, technical content, format, etc.) _____

BRL Report Number BRL-TR-3269 Division Symbol _____

Check here if desire to be removed from distribution list. ____

Check here for address change. ____

Current address: Organization _____
Address _____

DEPARTMENT OF THE ARMY
Director
U S Army Ballistic Research Laboratory
ATTN SLCBR-DD-T
Aberdeen Proving Ground, MD 21005-5066

OFFICIAL BUSINESS

BUSINESS REPLY MAIL
FIRST CLASS PERMIT No 0001, APG, MD

Postage will be paid by addressee

Director
U.S. Army Ballistic Research Laboratory
ATTN: SLCBR-DD-T
Aberdeen Proving Ground, MD 21005-5066

NO POSTAGE NECESSARY IF MAILED IN THE UNITED STATES